RF Breakdown and MAP

Daniel Bowring

Lawrence Berkeley National Laboratory,
Muon Accelerator Program

March 4, 2012

A statement of the problem

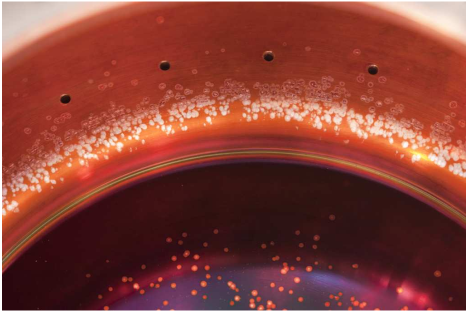

RF cavities in cooling channel conditions are limited by breakdown phenomena.

Strong magnetic fields limit cavity gradient.

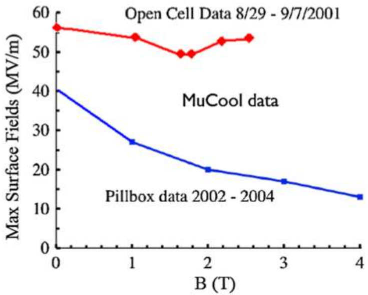

Figure: Maximum achievable gradient affected by magnetic field strength [Palmer et al., 2009].

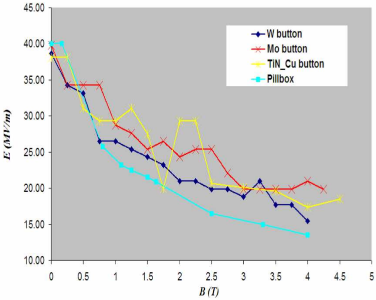

Figure: Similar phenomenon observable during button tests [Huang et al., 2007]. Coupler problems?

A few words of caution before we begin.

RF breakdown is a very interesting problem.

A few words of caution before we begin.

RF breakdown is a very interesting problem.

RF breakdown is a very *old* problem.

A few words of caution before we begin.

RF breakdown is a very interesting problem.

RF breakdown is a very *old* problem.

There is very likely no “magic bullet” solution.

A few words of caution before we begin.

RF breakdown is a very interesting problem.

RF breakdown is a very *old* problem.

There is very likely no “magic bullet” solution.

Our priority is a functioning cooling channel.

A General Picture Of Breakdown

The Conventional Picture

- Microscopic E-field enhanced to GV/m levels.
- Local F-N field emission currents approach 10^{11} A/m.
- Joule heating vaporizes surface features.
- Cu particles ionized by emitted e^{-}.
- Sheath forms, enables further emission.
- Explosion, melting, craters [Loew and Wang, 1999].

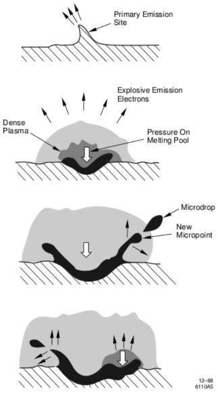

Figure: Cartoon of the emission process [Mesyats, 1983].

There are problems with the conventional picture.

- Empirical observation of frequency-dependence.
- $5 < \beta < 8$ measured.
  $40 < \beta < 60$ required by theory [Wang and Loew, 1989]. $\beta > 50$ not observed [Descoeudres, 2009].
- Geometric $\beta \sim h/r$. Hard to measure directly [Norem et al., 2003].
- Measuring $\langle j_{\mathrm{FN}} \rangle$ also imprecise.

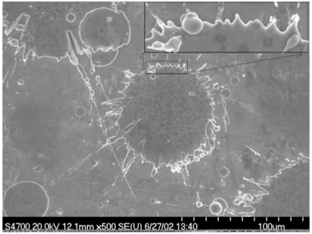

Figure: Damage area from open-cell 805 MHz cavity [Norem et al., 2003].

Things get very complicated, very quickly.

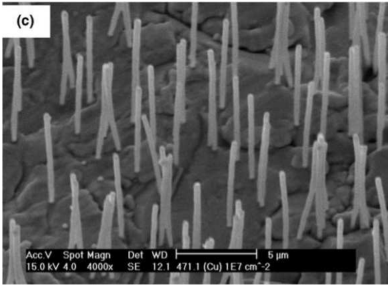

NOT FROM A CAVITY.

Cu nanowires grown, $\langle\beta\rangle = 245$ from FESM. Form factor predicts a factor of 3 lower. AND only 6% of them are strong emitters [Maurer et al., 2006].

A priori models are difficult.

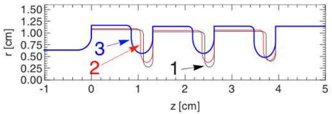

Figure: Vary geometry, study rf properties [Dolgashev et al., 2010].

- Test geometry-dependence of 11.242 GHz accelerating structures [Dolgashev et al., 2010].
- BD rate independent of fabricating lab, Cu type (OFHC, etc.).
- Surface treatment did *not* affect BD *rate*. Did improve conditioning time.

Correlation of geometry with RF properties (1)

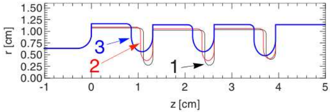

Figure: Vary geometry, study rf properties [Dolgashev et al., 2010].

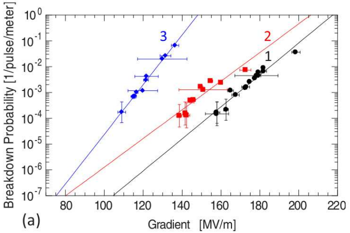

Figure: Gradient correlation with BD probability.

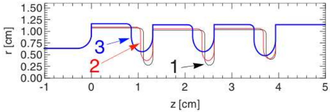

Figure: Vary geometry, study rf properties [Dolgashev et al., 2010].

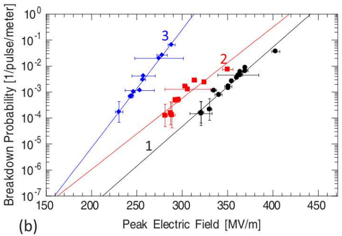

Figure: Peak electric field correlation with BD probability.

Correlation of geometry with RF properties (3)

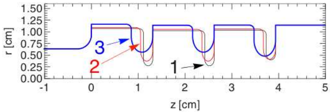

Figure: Vary geometry, study rf properties [Dolgashev et al., 2010].

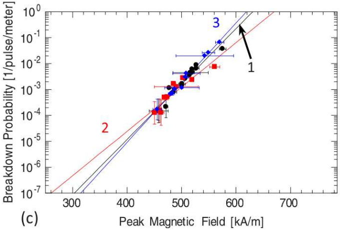

Figure: Peak magnetic field correlation with BD probability.

NB: It is *not* correct to say "magnetic field causes breakdown"!

Contribution of pulse length is also studied.

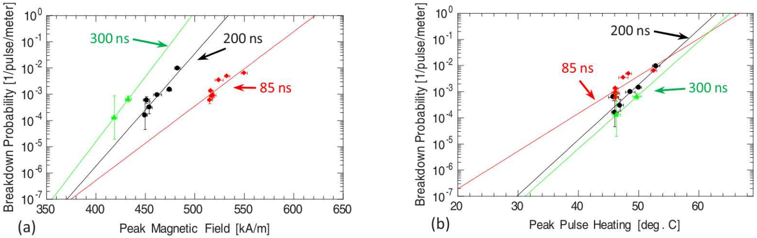

Varying pulse length shows strong correlation between BD probability and pulsed heating [Dolgashev et al., 2010].

Very recent work on pulsed heating looks promising.

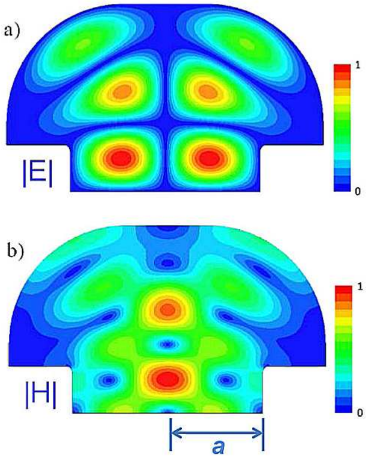

Figure: TE_{011} cavity has no surface electric fields, applies magnetic fields to small, removable samples [Laurent et al., 2011].

Pulsed heating experiments show material behavior.

[Laurent et al., 2011].

Mushroom cavity results

LISA LAURENT *et al.* Phys. Rev. ST Accel. Beams **14,** 041001 (2011)

TABLE I. Physical properties for the materials tested in this study and the pulsed heating ring width and minimum temperature where the onset of pulsed heating damage occurs.

Material	Heat capacity (J/kg/K)	Thermal conductivity (W/m/K)	Electrical conductivity % IACS	Density (gm)	Maximum pulsed heating temperature (Ho = 600 kA/m) (Celsius)	Pulsed heating ring width (mm)	Onset of pulsed heating damage (Celsius)
Copper (SLAC)	394	391	101[a]	8.94	110	10.7	66
SPDT Cu	394	391	(100)[b]	8.94	110	4.7	100
HIP2 Cu	394	391	(100)[b]	8.94	110	11.9	57
CuZr (annealed)	394	367	78–82[a]	8.89	114	12.1	58
CuCr (annealed)	385	324	83.5[a]	8.89	121	13.4	52
Single crystal Cu	394	391	(100)[b]	8.94	110	5.4	97
E-deposited Cu	394	391	(100)[b]	8.94	110	8.5	80
Silver plated Cu	233	429	(105)[b]	10.5	125	12.5	60
CuZr (cold worked)	394	367	82–83	8.89	114		>114
CuAg (SLAC)	385	346	97–100.1	8.89	117	6.2	100
CuAg (KEK)	385	346	97	8.89	117	4.7	107
CuCr (nonannealed)	385	324	83.5	8.89	121		>121
Glidcop	384	335	91.5	8.91	119		>119

[a]Precise information not available.
[b]Measured values prior to heat treatment.

Figure: Results from [Laurent et al., 2011].

Mushroom cavity results

LISA LAURENT *et al.* Phys. Rev. ST Accel. Beams **14,** 041001 (2011)

TABLE I. Physical properties for the materials tested in this study and the pulsed heating ring width and minimum temperature where the onset of pulsed heating damage occurs.

Material	Heat capacity (J/kg/K)	Thermal conductivity (W/m/K)	Electrical conductivity % IACS	Density (gm)	Maximum pulsed heating temperature (Ho = 600 kA/m) (Celsius)	Pulsed heating ring width (mm)	Onset of pulsed heating damage (Celsius)
Copper (SLAC)	394	391	101[a]	8.94	110	10.7	66
SPDT Cu	394	391	(100)[b]	8.94	110	4.7	100
HIP2 Cu	394	391	(100)[b]	8.94	110	11.9	57
CuZr (annealed)	394	367	78–82[a]	8.89	114	12.1	58
CuCr (annealed)	385	324	83.5[a]	8.89	121	13.4	52
Single crystal Cu	394	391	(100)[b]	8.94	110	5.4	97
E-deposited Cu	394	391	(100)[b]	8.94	110	8.5	80
Silver plated Cu	233	429	(105)[b]	10.5	125	12.5	60
CuZr (cold worked)	394	367	82–83	8.89	114		>114
CuAg (SLAC)	385	346	97–100.1	8.89	117	6.2	100
CuAg (KEK)	385	346	97	8.89	117	4.7	107
CuCr (nonannealed)	385	324	83.5	8.89	121		>121
Glidcop	384	335	91.5	8.91	119		>119

[a]Precise information not available.
[b]Measured values prior to heat treatment.

Figure: Results from [Laurent et al., 2011].

Mushroom cavity results

TABLE I. Physical properties for the materials tested in this study and the pulsed heating ring width and minimum temperature where the onset of pulsed heating damage occurs.

Material	Heat capacity (J/kg/K)	Thermal conductivity (W/m/K)	Electrical conductivity % IACS	Density (gm)	Maximum pulsed heating temperature (Ho = 600 kA/m) (Celsius)	Pulsed heating ring width (mm)	Onset of pulsed heating damage (Celsius)
Copper (SLAC)	394	391	101[a]	8.94	110	10.7	66
SPDT Cu	394	391	(100)[b]	8.94	110	4.7	100
HIP2 Cu	394	391	(100)[b]	8.94	110	11.9	57
CuZr (annealed)	394	367	78–82[a]	8.89	114	12.1	58
CuCr (annealed)	385	324	83.5[a]	8.89	121	13.4	52
Single crystal Cu	394	391	(100)[b]	8.94	110	5.4	97
E-deposited Cu	394	391	(100)[b]	8.94	110	8.5	80
Silver plated Cu	233	429	(105)[b]	10.5	125	12.5	60
CuZr (cold worked)	394	367	82–83	8.89	114		>114
CuAg (SLAC)	385	346	97–100.1	8.89	117	6.2	100
CuAg (KEK)	385	346	97	8.89	117	4.7	107
CuCr (nonannealed)	385	324	83.5	8.89	121		>121
Glidcop	384	335	91.5	8.91	119		>119

[a]Precise information not available.
[b]Measured values prior to heat treatment.

Figure: Results from [Laurent et al., 2011].

NB: This tells us nothing about field emission!

In Summary

- Even without strong magnetic fields, BD is difficult to understand.
- It's generally accepted that field emission plays a role in triggering breakdown events.
- Many cavities tested over many years, and still very little definitive knowledge of BD physics.

It's even harder for low-frequency cavities.

An observation: 201 MHz cavities are large and therefore expensive. How can we hope to approach this level of statistical understanding?

Field Emission Physics

Field Emission

Considering the Fowler-Nordheim equation:

$$\langle j \rangle = \frac{5.7 \times 10^{-12} \cdot 10^{4.52\phi^{-0.5}}}{\phi^{1.75}} (\beta E_s)^{2.5} \exp\left(-\frac{6.53 \times 10^9 \cdot \phi^{1.5}}{\beta E_s}\right)$$

- ϕ is the work function of the metal, measured in eV.
- It is usually taken as a constant.
- ϕ is not constant. It changes depending on grain orientation [Smoluchowski, 1941], and also depending on the local crystal strain [Chow and Tiller, 1984].
- An examination of variations in ϕ may resolve some of the inconsistencies involved in β-oriented measurements and calculations.

ϕ changes with surface structure.

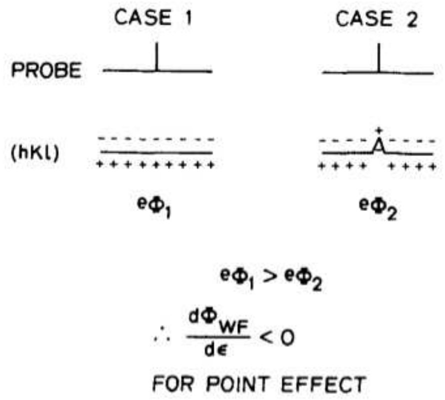

Figure: A qualitative argument that tips alter the surface dipole layer [Chow and Tiller, 1984]. (See paper for a quantitative argument.)

ϕ changes with fatigue cycling.

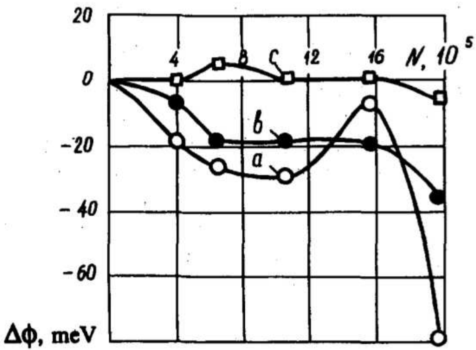

Fig. 2. The increment of the electronic work function for aluminium surface vs the number of cycles. (a) Area of a specimen directly above the future crack; (b) 1 mm from that area; (c) 3 mm from it.

Figure: $\Delta\phi$ used to predict fatigue damage [Levitin et al., 1994].

$\langle j \rangle$ vs. ϕ

The average work function of copper is ≈ 4.5 eV.

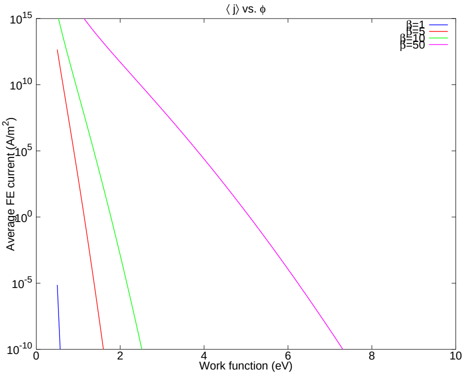

Figure: Average FE current for varying work function, using 4 different values of β. $E = 50$ MV/m.

MAP-Specific Issues

Breakdown in strong magnetic fields is even less well understood.

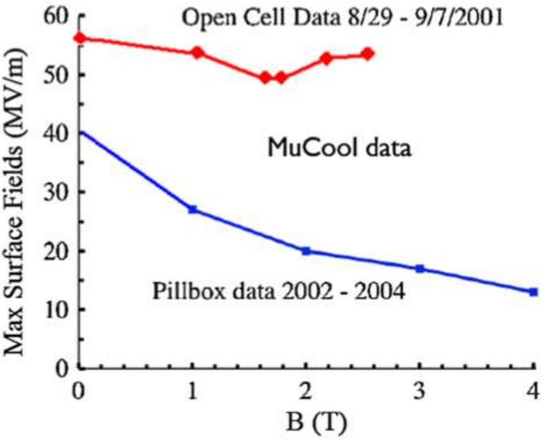

Figure: Maximum achievable gradient affected by magnetic field strength [Palmer et al., 2009].

Theory: Beamlet focusing.

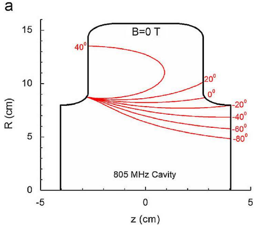

Figure: Emitted e$^-$ path, $B = 0$ T.

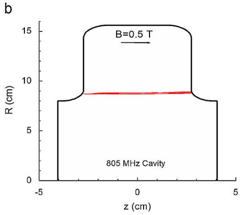

Figure: Emitted e$^-$ path, $B = 0.5$ T.

- Field emission from surface defects.
- Emitted electrons focused into “beamlet” by solenoidal B-fields.
- Beamlet heats opposite surface, causing fatigue, damage.
- Damage instigates breakdown [Stratakis et al., 2010].

Beamlets create pulsed heating effect on opposite wall.

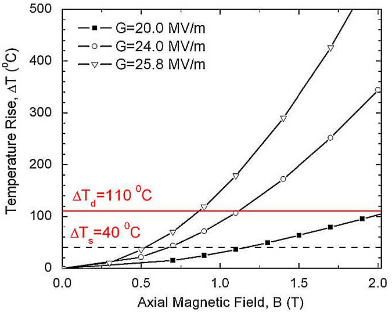

Figure: Temperature rise vs. magnetic field strength for various gradients [Stratakis et al., 2010]. Please recall [Laurent et al., 2011].

NB: Experience with X-band structures suggests $\Delta T < 50$ K is a "safe" operating point. Not much experience to inform < 1 GHz operation.

A few experiments are possible here.

- Beryllium wall cavity experiments (see Derun Li's talk)
- "Anti-button" tests suppress FE in beamlet damage region (see cartoon).

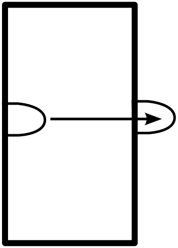

Briefly, we observe damage consistent with this model.

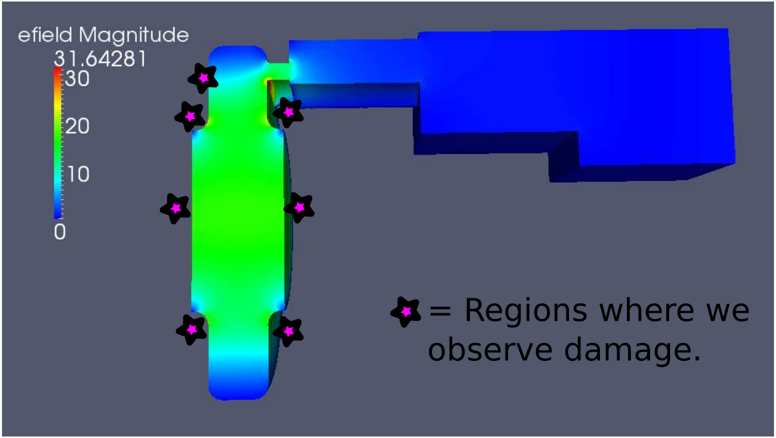

Figure: Current 805 MHz cavity. Electric field modeled using ACE3P.

Modeling Breakdown

- A localized "plasma spot" in the cavity may explain behavior during breakdown [Dolgashev and Tantawi, 2002].
- Ions, clusters in the cavity trigger this process.
- These particles have several possible sources [Norem et al., 2005]:
  - Fracture / field evaporation: E-field tensile stresses pull Cu atoms off surface.
  - Surface currents + surface defects $\rightarrow$ large field enhancements.
- Ionization of clusters from field-emitted electrons.

Given the complexity of the cavity surface (grain boundaries, asperities, etc.) one can imagine this getting very complicated, very quickly.

Experimental apporach: atomic layer deposition.

Several aspects of this model require field enhancements at a rough surface. Fix this with ALD.

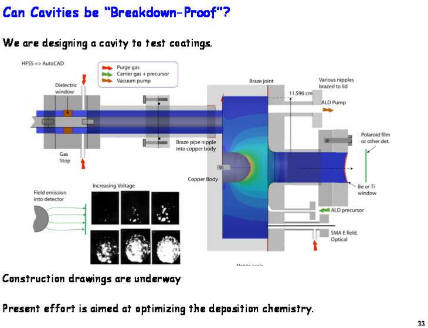

Figure: [Norem, 2011]

Computational approach: PIC, MD simulations

A clear understanding of the breakdown process may suggest surface treatments, material choices.

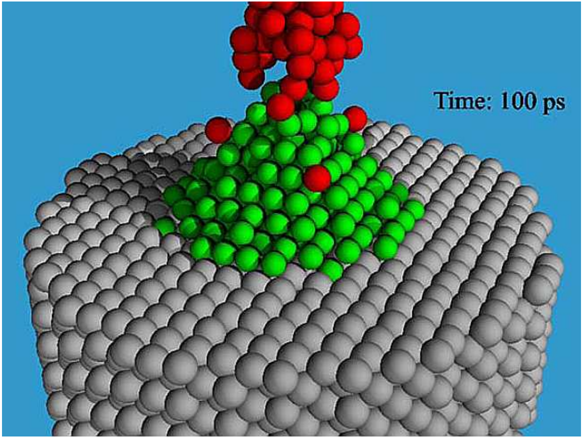

Figure: [Norem et al., 2005]

Change stored energy in cavity to change plasma properties.

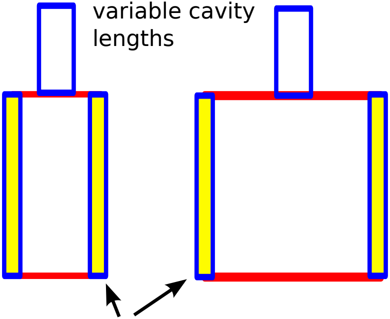

This sort of test is possible with the new modular Be wall cavity design. (See D. Li's talk.)

The magnetoplastic effect

Strong DC magnetic fields can influence the plasticity of even non-ferrous metals!

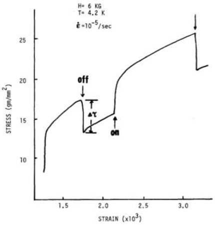

FIG. 2. The influence of a change in the magnetic field on the flow stress of a copper crystal; the crystal is oriented for so-called easy glide. Note the reversibility, which rules out the possibilty that the effect is related to eddy currents. We also note that the yield stress, τ_y, of the crystal is given as 0.9 kg/mm^2.

Figure: Magnetic field changes flow stress in Cu [Galligan et al., 1977].

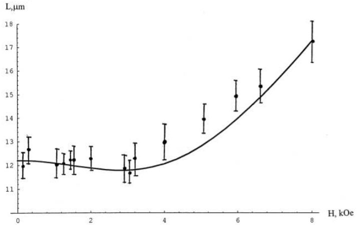

Figure: Applied B-field changes dislocation path length [Molotskii and Fleurov, 2000].

The magnetoplastic effect

Why? B-field changes spin multiplicity in dangling dislocation end bonds. Increase in fraction of occupied triplet states with lower binding energy. This increases plasticity [Molotskii, 2000].

Dislocation motion is inhibited via, e.g., solid solution hardening. See [Laurent et al., 2011].

Quantifying $< j_{\mathrm{FN}} >$ vs. B

1-button experiments using a Faraday cup. This should be coupled with careful surface analysis.

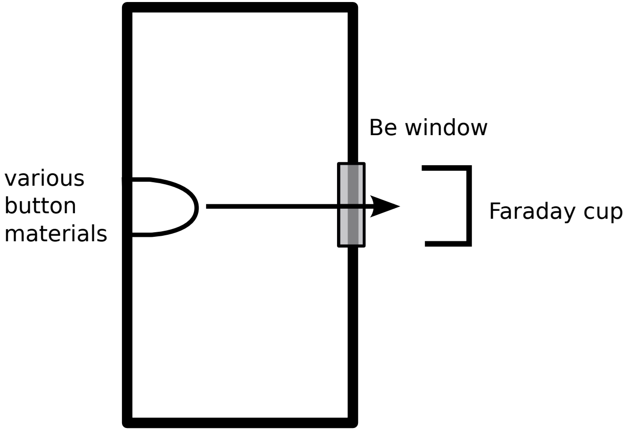

Conclusions

- Complex subject + short talk → I've left out a lot of interesting stuff.
- Many good experiments possible.
- Growing consensus: The cavity surface is not simple.
- No need to pick only one BD model. Why should these processes be exclusive?
- What experimental choices advance the cause of a cooling channel?

Acknowledgements

Thanks to Zenghai Li for sending me the geometry of the 805 MHz pillbox cavity.

Thanks to the following people for interesting and helpful discussions: Chris Adolphsen, Valery Dolgashev, Derun Li, Jim Norem, Bob Palmer, Yagmur Torun.

Bibliography

Bibliography I

Antoine, C., P.auger, F., and Le Pimpec, F. (2011).
Electromigration occurrences and its effects on metallic surfaces submitted to high electromagnetic field: A novel approach to breakdown in accelerators.
Nucl. Inst. Meth. Phys. A, 665:54–69.

Chow, R. and Tiller, W. (1984).
Deformation-induced work function changes in cu single crystals. ii. theory.
J. Appl. Phys., 55(5):1346–1352.

Descoeudres, A. (2009).
Investigation of the dc vacuum breakdown mechanism.
PRST-AB, 12(092001).

Bibliography II

Dolgashev, V. et al. (2010).
Geometric dependence of radio frequency breakdown in normal conducting accelerating structures.
Appl. Phys. Lett., 97(171501).

Dolgashev, V. and Tantawi, S. (2002).
Rf breakdown in x-band waveguides.
In *Proc. EPAC 2002*, Paris, France.

Galligan, J., Lin, T., and Pang, C. (1977).
Electron-dislocation interaction in copper.
Phys. Rev. Lett., 38(8):405–407.

Huang, D. et al. (2007).
805 mhz cavity button test.
In *MTA RF Workshop*. FNAL.

Bibliography III

Koller, L. and Johnson, R. (1937).
Visual observations of the malter effect.
Phys. Rev., 32:519–523.

Laurent, L. et al. (2011).
Experimental study of rf pulsed heating.
PRST-AB, 14(041001):1–21.

Levitin, V. et al. (1994).
influence of cyclic stresses upon the electronic work function for the metal surface.
Solid State Communications, 92(12):973–976.

Loew, G. and Wang, J. (1999).
Handbook of Aceelerator Physics and Engineering.
World Scientific, Hackensack, NJ, USA, 3rd edition.

Bibliography IV

Malter, L. (1941).
The behavior of electrostatic electron multipliers as a function of frequency.
Proc. I.R.E., 29(11):587–598.

Maurer, F. et al. (2006).
Field emission of copper nanowires grown in polymer ion-track membranes.
Nucl. Inst. Meth. Phys. B, 245(1):337–341.

Mesyats, G. (1983).
Explosive proceses on the cathode in a vacuum discharge.
IEEE Trans. on Electrical Insulation, EI-18(3):218–225.

Bibliography V

Molotskii, M. (2000).
Theoretical basis for electro- and magnetoplasticity.
Mat. Sci. Eng., A287:248–258.

Molotskii, M. and Fleurov, V. (2000).
Dislocation paths in a magnetic field.
J. Phys. Chem. B, 104(16):3812–3816.

Norem, J. (2011).
Modeling of arc and arc damage.
In *Joint MAP & High Gradient RF Collaboration Workshop*, Berkeley, CA.

Bibliography VI

Norem, J. et al. (2003).
Dark current, breakdown, and magnetic field effects in a multicell, 805 mhz cavity.
PRST-AB, 6(072001).

Norem, J., Insepov, Z., and Konkashbaev, I. (2005).
Triggers for rf breakdown.
Nucl. Inst. Meth. Phys. A, 537:510–520.

Palmer, R. et al. (2009).
rf breakdown with external magnetic fields in 201 and 805 mhz cavities.
PRST-AB, 12(031002):1–13.

Bibliography VII

Smoluchowski, R. (1941).
Anisotropy of the electronic work function of metals.
Phys. Rev., 60:661–674.

Stratakis, D., Gallardo, J., and Palmer, R. (2010).
Effects of external magnetic fields on the operation of high-gradient accelerating structures.
Nucl. inst. Meth. A, 620:147–154.

Wang, J. and Loew, G. (1989).
Rf breakdown studies in copper electron linac structures.
In *Proc. PAC 1989*, pages 1137–1139. IEEE.

Supplemental Slides

An cartoon showing precipitation hardening

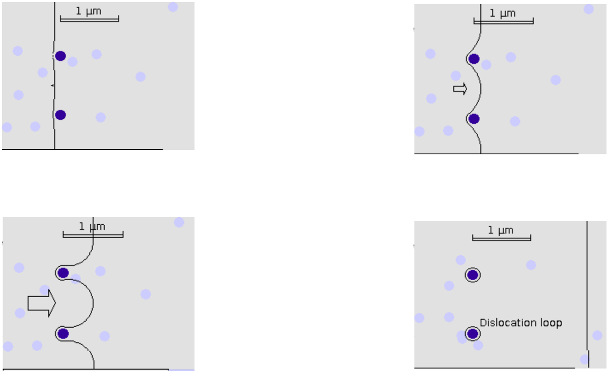

http://aluminum.matter.org.uk, by the European Aluminum Association and the University of Liverpool.

What other mechanisms may possibly contribute to RF breakdown?

Other mechanisms for future thought

- **Malter effect**: Enhanced secondary electron yield from oxide, contamination on conductor surface [Malter, 1941, Koller and Johnson, 1937].
- **Electromigration**: Large surface currents contribute to surface deformation [Antoine et al., 2011].